

Portland State University

PDXScholar

Civil and Environmental Engineering Faculty
Publications and Presentations

Civil and Environmental Engineering

4-21-2022

Robust Multi-Period Maximum Coverage Drone Facility Location Problem Considering Coverage Reliability

Darshan Rajesh Chauhan

Portland State University, drc9@pdx.edu

Avinash Unnikrishnan

Portland State University, uavinash@pdx.edu

Miguel A. Figliozzi

Portland State University, figliozzi@pdx.edu

Stephen D. Boyles

The University of Texas at Austin, sboyles@austin.utexas.edu

Follow this and additional works at: https://pdxscholar.library.pdx.edu/cengin_fac



Part of the [Transportation Engineering Commons](#)

Let us know how access to this document benefits you.

Citation Details

Published as: Chauhan, D. R., Unnikrishnan, A., Figliozzi, M. G., & Boyles, S. D. (2022). Robust Multi-Period Maximum Coverage Drone Facility Location Problem Considering Coverage Reliability. Transportation Research Record: Journal of the Transportation Research Board.

This Post-Print is brought to you for free and open access. It has been accepted for inclusion in Civil and Environmental Engineering Faculty Publications and Presentations by an authorized administrator of PDXScholar. Please contact us if we can make this document more accessible: pdxscholar@pdx.edu.

1 **Robust Multi-Period Maximum Coverage Drone Facility Location Problem Considering**
2 **Coverage Reliability**

3
4
5

6 **Darshan R. Chauhan**

7 Ph.D. Student and Graduate Research Assistant, Department of Civil and Environmental
8 Engineering,
9 Portland State University, Portland, OR 97201
10 Email: drc9@pdx.edu (Corresponding Author)

11

12 **Avinash Unnikrishnan**

13 Professor, Department of Civil and Environmental Engineering,
14 Portland State University, Portland, OR 97201
15 Email: uavinash@pdx.edu

16

17 **Miguel A. Figliozzi**

18 Professor, Department of Civil and Environmental Engineering,
19 Portland State University, Portland, OR 97201
20 Email: figliozzi@pdx.edu

21

22 **Stephen D. Boyles**

23 Associate Professor, Department of Civil, Architectural and Environmental Engineering,
24 The University of Texas at Austin, Austin, TX 78712
25 Email: sboyles@austin.utexas.edu

26

27

28

29

30 Word Count: 7396 words + 3 table(s) \times 250 = 8146 words

31

32

33

34

35

36

37 Submission Date: May 31, 2022

1 ABSTRACT

2 This study proposes a multi-period facility location formulation to maximize coverage
3 while meeting a coverage reliability constraint. The coverage reliability constraint is a chance-
4 constraint limiting the probability of failure to maintain the desired service standard, commonly
5 followed by emergency medical services and fire departments. Further, uncertainties in the fail-
6 ure probabilities are incorporated by utilizing robust optimization using polyhedral uncertainty
7 sets, which results in a compact mixed-integer linear program. A case study in the Portland, OR
8 metropolitan area is analyzed for employing unmanned aerial vehicles (UAVs) or drones to deliver
9 defibrillators in the region to combat out-of-hospital cardiac arrests. In our context, multiple peri-
10 ods represent periods with different wind speed and direction distributions. The results show that
11 extending to a multi-period formulation, rather than using average information in a single period,
12 is particularly beneficial when either response time is short or uncertainty in failure probabilities is
13 not accounted for. Accounting for uncertainty in decision-making improves coverage significantly
14 while also reducing variability in simulated coverage, especially when response times are longer.
15 Going from a single-period deterministic formulation to a multi-period robust formulation boosts
16 the simulated coverage values by 57%, on average. The effect of considering a distance-based
17 equity metric in decision-making is also explored.

1 INTRODUCTION

2 Public service agencies like hospitals, fire, rescue, and police departments are required to
3 maintain high levels of service. For example, fire-related incidents require 90% reliability for a
4 4-minute response time (1). Similarly, in the case of emergency medical services, the US Emer-
5 gency Medical Services Act of 1997 requires a 95% response rate within 10 minutes (2). In the
6 United Kingdom, the National Health Service aims at serving 75% and 95% of demands in 8 and
7 14 minutes, respectively (3). As transportation systems are dynamic and stochastic an inherent
8 uncertainty in travel time is present. This uncertainty in travel time leads to uncertainty in facility
9 or demand coverage.

10 Drone or unmanned aerial vehicle (UAV) deliveries are being explored as a quicker, more
11 cost-effective, and more reliable alternative for time-sensitive medical deliveries, emergency sce-
12 narios, humanitarian logistics, and other agricultural, security, and military applications (4, 5).
13 Large corporations such as Amazon have secured operational licenses and begun field trials (6). In
14 addition, there is support from federal programs, such as the Federal Aviation Authority's UAS-
15 BEYOND program (7), to test medical applications including delivery of automatic external defib-
16 rillators (AEDs), medical prescriptions, and medical emergency response. These medical applica-
17 tions are being field tested in the states of Nevada, North Carolina, and North Dakota, respectively.

18 Drones have some advantages when compared to traditional ground transportation modes.
19 They can arrive faster by taking more direct paths and avoiding ground-based obstructions or
20 congestion. For ground vehicles, congestion and associated delays are key sources of travel time
21 uncertainty. But for drone deliveries uncertainties arise because of weather conditions, mainly
22 from uncertainty about wind speed and direction (8).

23 The effect of stochasticity in environmental factors on the performance of emergency de-
24 partments is hard to quantify exactly, in addition to being data-intensive. However, reliable esti-
25 mates for expected values (like, mean and variance) and extrema (like, minimum and maximum)
26 are much easier to obtain. This is much more true for strategic decisions like facility location when
27 the planning periods are longer. Robust optimization (RO) is a distribution-free approach that al-
28 lows for incorporating stochasticity with limited information using uncertainty sets. The splitting
29 of a planning period into multiple smaller periods would disaggregate uncertainties and possibly
30 aid RO in tackling them.

31 This paper considers a robust multi-period maximum coverage facility location problem
32 considering coverage reliability (MP-R) to improve decision-making. The coverage reliability
33 constraints are captured using the chance constraints which provide probabilistic constraint satis-
34 faction guarantee. The final model is developed by integrating the chance constrained approach
35 with robust optimization, similar to Lutter et al. (2), and expanded to multiple time periods. The
36 contributions of this paper are:

- 37 • Developing a compact mixed-integer linear programming formulation for MP-R using
38 polyhedral uncertainty sets (9).
- 39 • Developing a case study in the Portland, OR metropolitan area to locate drone-launch
40 sites to deliver defibrillators, considering uncertainty in travel times arising due to varia-
41 tion in wind speeds and directions.
- 42 • Analyzing the value of adding robustness and multiple time periods using a novel Monte-
43 Carlo simulation scheme.

44 A brief literature review is presented in the next section, followed by the development of the
45 mathematical model. The case study is developed and the computational analyses are discussed.

1 Finally, the paper ends with brief conclusions and recommendations for future research.

2 **LITERATURE REVIEW**

3 A plethora of research has already been conducted in the field of emergency medical re-
4 sponse. A vast majority of research has been focused around using ground vehicles (i.e., tradi-
5 tional ambulances) for optimizing coverage (10–13), survival rates (14, 15), amount of relocation
6 (10, 13, 16), and crew shifts (11). Detailed literature reviews on ambulance location can be found
7 in (17–19). Recently, there has been increasing interest around the usage of air-based vehicles for
8 emergency medical operations: AED-enabled drones for out-of-hospital cardiac arrests (20, 21),
9 drones supplying emergency relief packages (22, 23), helicopters (24), and air ambulances (25).
10 This study focuses on locating AED-enabled drones for tackling out-of-hospital cardiac events
11 in a planning region using a multi-period facility location formulation incorporating reliability in
12 coverage.

13 Multi-period variants of traditional facility location problems have been studied for various
14 contexts since the seminal work of Ballou (26). Nickel and da Gama (27) provides a review of
15 multi-period facility location problems (MPFLP), and Vatsa and Jayaswal (28) provides a brief
16 review of studies considering uncertainties in MPFLP literature. Vatsa and Jayaswal (28) note that
17 while demand and cost uncertainties are widely tackled in the MPFLP literature, research tackling
18 supply-side uncertainties (example, coverage capabilities) is relatively scarce. Kim et al. (29)
19 propose a MPFLP with drones considering uncertainty in flight distances. The study assumes that
20 the probability of drone’s successful return to the launch station is not time-period-dependent and
21 that the time-periods are long enough that all drone trips complete in a time-period. Ghelichi et al.
22 (30) proposes a multi-stop drone location and scheduling problem for medical supply delivery. The
23 study assumes deterministic travel speed for drones (i.e., ignoring weather conditions) in multiple
24 periods, and time-periods are short and a drone-trip is assumed to last over multiple time periods.
25 Our study assumes that the probability of timely arrival at a demand location from a launch site is
26 dependent on the time period, and that the time-periods are long enough that drones trips can be
27 completed in a time period.

28 Erdoğan et al. (11) state that appropriately defining coverage and incorporating uncertainty
29 in travel times are the most important considerations in ambulance location. This study defines
30 coverage based on the importance of covering the demand point. Therefore, the coverage impor-
31 tance metric can be a function of various population parameters like size and demographics, and
32 other characteristics like history of emergency requests and equity considerations. Additionally, in
33 most regions, the emergency response systems are required to maintain adequate service standards.
34 We model the service standard reliability constraint as a chance constraint on probability of timely
35 arrival for each demand point. Therefore, a demand point is considered covered only if the service
36 standard reliability requirements are met for all time periods of the planning period.

37 The probability of timely arrival at a demand point is linked to the uncertainty in drone
38 travel times which stems from variations in wind speed and directions. Due to dependency on
39 environmental factors, the estimated values of probabilities of timely arrival are not deterministic,
40 rather uncertain. Tackling parameter uncertainty has been a focus of the mathematical program-
41 ming community for a long time. Two major approaches exist for tackling uncertainty: stochastic
42 optimization (SO) and robust optimization (RO). SO assumes that a probability distribution of the
43 uncertainty is available, whereas RO assumes no underlying distribution of the uncertainty and con-
44 siders it to be deterministic and set-based (31, 32). A set-based uncertainty structure of RO leads to

1 better computational tractability than SO (32). RO immunizes the solution from any manifestation
 2 of uncertainty in the described uncertainty set. In general, the larger the size of the uncertainty set,
 3 the lower is the objective value (considering maximization objective) and the lower is the proba-
 4 bility of constraint violation (32). This trade-off between expected objective values and constraint
 5 violation can be controlled by varying the size of the uncertainty set. Here, we use RO using poly-
 6 hedral uncertainty sets (9) to tackle uncertainty while maintaining computational tractability. This
 7 approach ensures that the robust counterpart of our linear optimization problem is also linear. We
 8 refer the interested reader to (31–36) for a more comprehensive picture of RO.

9 PROBLEM DESCRIPTION

10 This section first describes the modeling of the coverage reliability constraint and its as-
 11 sumptions. Later, we formulate a deterministic multi-period maximum coverage facility location
 12 problem with coverage reliability (abbreviated as MP-D). Finally, we provide a robust formulation
 13 of MP-D (abbreviated as MP-R) which accounts for uncertainty in the values of coverage failure
 14 probabilities.

15 Consider a set of demand points (represented as I) each with coverage importance c_i , a set
 16 of facilities (represented as J), and a set of all time periods (represented as T). Let A be a $|I| \times |J|$
 17 1-0 accessibility matrix describing if the demand point i can be covered by a facility j . We use a_{ij}^t
 18 to represent the probabilistic nature of the (i, j) element of A in time period $t \in T$, while, A_{ij} is
 19 used for the deterministic initial state of (i, j) element of the matrix A . More specifically, if $A_{ij} = 1$,
 20 then, $a_{ij}^t = 1$ with probability $(1 - p_{ij}^t)$, and $a_{ij}^t = 0$ with probability p_{ij}^t . If $A_{ij} = 0$, then, $a_{ij}^t = 0$
 21 always. Let, \bar{p}_{ij}^t be our estimate of p_{ij}^t . Now, the service reliability requirement of achieving a
 22 service standard α can then be stated as

$$23 \Pr \left[\sum_{j \in S_i} a_{ij}^t \geq 1 \right] \geq \alpha, \quad (1)$$

24 where $S_i = \{j \in J | A_{ij} = 1\}$. The above equation potentially considers all the facilities that can
 25 access demand point $i \in I$. As a consequence, we assume that all the accessible facilities respond
 26 to the demand at location i . Under the assumption of independence among the values in A , equation
 27 (1) can be modified as

$$Pr \left[\sum_{j \in S_i} a_{ij}^t \geq 1 \right] = 1 - \prod_{j \in S_i} p_{ij}^t \equiv 1 - \prod_{j \in S_i} \bar{p}_{ij}^t \geq \alpha \quad (2)$$

28 For the above discussion, we have assumed that \bar{p}_{ij}^t completely describe the distribution
 29 of variables a_{ij}^t . However, there are errors endemic to sampling (environmental factors) and mea-
 30 surement while estimating the value of p_{ij}^t . Therefore, the values of p_{ij}^t may not be known with
 31 complete certainty. We tackle this issue while formulating the MP-R model.

32 For MP-D and MP-R, the decision-making agency wishes to locate a maximum of q fa-
 33 cilities in each time-period to maximize the cumulative coverage importance achieved subject to
 34 coverage requirements described. Additionally, opened facility locations can be shifted between
 35 time periods subject to a facility relocation cost budget constraint.

1 Nomenclature

Sets and Indices

- 1 I Set of all demand points ($i \in I$)
 2 J Set of all candidate facility locations ($j, k \in J$)
 T Set of all time periods ($t \in T := \{1, 2, \dots, |T|\}$)

Parameters

- c_i Coverage importance of demand point $i \in I$; $c_i \geq 0$
 A_{ij} 1, if the demand point $i \in I$ can be covered by facility $j \in J$, and 0, otherwise
 S_i Set of facilities $j \in J$ that can cover the demand point $i \in I$; $S_i = \{j \in J | A_{ij} = 1\} \forall i \in I$
 \bar{p}_{ij}^t Nominal probability of failure of covering demand point $i \in I$ by facility $j \in J$ in time period $t \in T$; $0 < \bar{p}_{ij}^t \leq 1$
 3 \hat{p}_{ij}^t Maximum deviation from nominal probability of failure of covering demand point $i \in I$ by facility $j \in J$ in time period $t \in T$; $0 \leq \hat{p}_{ij}^t < \bar{p}_{ij}^t + \hat{p}_{ij}^t \leq 1$
 q Maximum number of facilities that can be located; $q \in \mathbb{Z}^+ \cup \{0\}$
 α Required coverage threshold; $0 \leq \alpha \leq 1$
 Γ_i^t Maximum number of delivery paths to demand point i that can achieve worst-case probability of failure simultaneously in time period $t \in T$; $\Gamma_i^t \in \mathbb{Z}^+ \cup \{0\}$
 f_{jk}^t Cost associated with shifting the facility from location $j \in J$ to location $k \in J$ at the beginning of time period $t \in T$
 B Facility shifting cost budget

Decision Variables

- x_i 1, if demand location $i \in I$ is covered with given coverage threshold; 0, otherwise
 4 y_j^t 1, if candidate facility location $j \in J$ is open during time period $t \in T$; and 0, otherwise
 z_{jk}^t 1, if a facility is moved from location $j \in J$ to location $k \in J$ at the beginning of time period $t \in T \setminus \{1\}$; and 0, otherwise

5 Deterministic Formulation

$$\max_{x,y,z} \sum_{i \in I} c_i x_i \quad (3)$$

$$\prod_{j \in S_i} (\bar{p}_{ij}^t)^{y_j^t} \leq (1 - \alpha)^{x_i} \quad \forall i \in I, t \in T \quad (4)$$

$$\sum_{j \in J} y_j^t \leq q \quad \forall t \in T \quad (5)$$

$$\sum_{t \in T \setminus \{1\}} \sum_{j \in J} \sum_{k \in J} f_{jk}^t z_{jk}^t \leq B \quad (6)$$

$$\sum_{k \in J} z_{jk}^t = y_j^{t-1} \quad \forall j \in J, t \in T \setminus \{1\} \quad (7)$$

$$\sum_{j \in J} z_{jk}^t = y_k^t \quad \forall k \in J, t \in T \setminus \{1\} \quad (8)$$

$$x_i \in \{0, 1\} \quad \forall i \in I \quad (9)$$

$$y_j^t \in \{0, 1\} \quad \forall j \in J, t \in T \quad (10)$$

$$z_{jk}^t \in \{0, 1\} \quad \forall j, k \in J, t \in T \setminus \{1\} \quad (11)$$

1 For the deterministic formulation, we assume that $p_{ij}^t = \bar{p}_{ij}^t$. Equation (3) represents maximizing
 2 coverage importance. In equation (4), the demand point $i \in I$ is covered only if the probability
 3 of failure to cover it is less than $(1 - \alpha)$ for all time periods $t \in T$. Note that all accessible open
 4 facilities respond to meet the demand at point $i \in I$. Equation (5) enforces that no more than q
 5 facilities can be opened.

6 Equation (6) is a generalized cost constraint relating to the shifting facility locations. Equa-
 7 tions (7) and (8) are transportation allocation constraints. Note that using $f_{jj}^t = 0$ for all $j \in J, t \in$
 8 $T \setminus \{1\}$, and 1, otherwise, would limit the total number of facility location shifts to B . Equations
 9 (9)–(11) are variable definitions. However, the formulation is not linear due to equation (4). Ap-
 10 plying logarithm function on both sides of equation (4) yields:

$$\sum_{j \in S_i} w_{ij}^t y_j^t \leq \beta x_i \quad \forall i \in I, t \in T \quad (12)$$

11 where w_{ij}^t and β represent $\log(\bar{p}_{ij}^t)$ and $\log(1 - \alpha)$, respectively. The above formulation (equations
 12 3 and 5–12) is referred to as the deterministic multi-period facility location problem considering
 13 coverage reliability, abbreviated as MP-D. MP-D is an integer linear program and can be solved
 14 using standard MIP solvers.

15 **Robust Formulation**

16 The parameter p_{ij}^t represents the probability that the facility $j \in J$, in time period $t \in T$, will fail
 17 to cover the demand point $i \in I$ in a given service time threshold τ . However, due to sampling
 18 errors stemming from environmental factors like variations in travel times throughout the day, the
 19 estimated values of parameters p_{ij}^t are uncertain. Later, in the presented case study of delivering
 20 AED-enabled drones, this variation occurs primarily due to changing wind speeds and directions.
 21 As the complete probability distribution of p_{ij}^t is arduous to obtain in comparison to the bounds
 22 of its variation, we use a robust optimization using polyhedral uncertainty sets (9) to incorporate
 23 this uncertainty. Let, \hat{p}_{ij}^t be the maximum deviation of \bar{p}_{ij}^t . For our robust model, we assume that
 24 $p_{ij}^t \in [\bar{p}_{ij}^t - \hat{p}_{ij}^t, \bar{p}_{ij}^t + \hat{p}_{ij}^t]$. Of all facilities servicing demand point i , up to Γ_i^t facilities observe
 25 worst-case failure probabilities (i.e., $p_{ij}^t = \bar{p}_{ij}^t + \hat{p}_{ij}^t$), whereas the rest observe nominal failure
 26 probabilities (i.e., $p_{ij}^t = \bar{p}_{ij}^t$). This allocation happens in such a way that the probability of failing
 27 to serve demand point i is maximized.

$$\max_{x,y,z} \sum_{i \in I} c_i x_i \quad (13)$$

$$\max_{\{U \subseteq S_i, |U| \leq \Gamma_i\}} \left[\prod_{j \in U} (\bar{p}_{ij}^t + \hat{p}_{ij}^t)^{y_j^t} \prod_{j \in S_i \setminus U} (\bar{p}_{ij}^t)^{y_j^t} \right] \leq (1 - \alpha)^{x_i} \quad \forall i \in I, t \in T \quad (14)$$

$$\sum_{j \in J} y_j^t \leq q \quad \forall t \in T \quad (15)$$

$$\sum_{t \in T \setminus \{1\}} \sum_{j \in J} \sum_{k \in J} f_{jk}^t z_{jk}^t \leq B \quad (16)$$

$$\sum_{k \in J} z_{jk}^t = y_j^{t-1} \quad \forall j \in J, t \in T \setminus \{1\} \quad (17)$$

$$\sum_{j \in J} z_{jk}^t = y_k^t \quad \forall k \in J, t \in T \setminus \{1\} \quad (18)$$

$$x_i \in \{0, 1\} \quad \forall i \in I \quad (19)$$

$$y_j^t \in \{0, 1\} \quad \forall j \in J, t \in T \quad (20)$$

$$z_{jk}^t \in \{0, 1\} \quad \forall j, k \in J, t \in T \setminus \{1\} \quad (21)$$

1 Equation (13) represents the maximization of coverage importance. Incorporating uncer-
 2 tainty in the failure probabilities in equation (4) yields (14). The left hand side (lhs) of equation
 3 (14) seeks to find the absolute worst-case probability of failure such that at most Γ_i facilities ser-
 4 vicing the demand point $i \in I$ can individually observe worst-case failure probability. Demand
 5 point $i \in I$ is considered covered only if the left-hand side of equation (14) is less than $(1 - \alpha)$.
 6 Generally, incorporating robustness into a problem imparts conservatism by realizing worst-case
 7 objective value subject to certain criteria (9, 37). This leads to the robustness sub-problem being
 8 in conflict with the overall objective. Here, worst-case realizations of failure probability in equa-
 9 tion (14) reduce the chance of the demand point i being covered, and while the overall objective
 10 (13) want to increase the chances of demand point i being covered. In other words, the current
 11 formulation is a bilevel optimization problem which cannot be solved directly using MIP solvers.
 12 Dualizing the robustness sub-problem would overcome this issue and align both objectives cor-
 13 rectly, and yield a single level mixed-integer linear problem. Equations (15)-(21) have the same
 14 meaning as equations (5)-(11). Taking the logarithm of (14) yields:

$$\max_{\{U \subseteq S_i, |U| \leq \Gamma_i\}} \left[\sum_{j \in U} \log(\bar{p}_{ij}^t + \hat{p}_{ij}^t) \cdot y_j^t + \sum_{j \in S_i \setminus U} \log(\bar{p}_{ij}^t) \cdot y_j^t \right] \leq \log(1 - \alpha) \cdot x_i \quad \forall i \in I, t \in T \quad (22)$$

15 Let, \hat{w}_{ij}^t , w_{ij}^t , and β represent $\log(\bar{p}_{ij}^t + \hat{p}_{ij}^t)$, $\log(\bar{p}_{ij}^t)$, and $\log(1 - \alpha)$, respectively. Note
 16 that $\hat{w}_{ij}^t \geq w_{ij}^t$. Rewriting \hat{w}_{ij}^t as $w_{ij}^t + (\hat{w}_{ij}^t - w_{ij}^t)$, we re-write equation (22) as:

$$\sum_{j \in S_i} w_{ij}^t y_j^t + \max_{\{U \subseteq S_i, |U| \leq \Gamma_i\}} \left[\sum_{j \in U} (\hat{w}_{ij}^t - w_{ij}^t) \cdot y_j^t \right] \leq \beta x_i \quad \forall i \in I, t \in T \quad (23)$$

17 The optimization problem described on the lhs of equation (23) can be written as:

For each $i \in I, t \in T$:

$$SP_i^t : \quad \max_{\gamma} \quad \sum_{j \in S_i} w_{ij}^t y_j^t + \sum_{j \in S_i} (\hat{w}_{ij}^t - w_{ij}^t) y_j^t \gamma_{ij} \quad (24)$$

$$\sum_{j \in S_i} \gamma_{ij} \leq \Gamma_i^t \quad (25)$$

$$\gamma_{ij} \in \{0, 1\} \quad \forall j \in S_i \quad (26)$$

1 The constraint coefficient matrix of the above sub-problem is totally unimodular, and Γ_i^t
 2 are non-negative integer values. Therefore, γ_{ij}^t can be linearized to the interval $[0,1]$ without loss
 3 of optimality. Let, θ_i^t and σ_{ij}^t be the dual variables associated with equations (25) and the upper
 4 bound of equation (26), respectively. Taking the dual of the formulation represented by equations
 5 (24)-(26), yields:

For each $i \in I, t \in T$:

$$SPD_i^t : \quad \min_{\sigma, \theta} \quad \sum_{j \in S_i} w_{ij}^t y_j^t + \sum_{j \in S_i} \sigma_{ij}^t + \Gamma_i^t \theta_i^t \quad (27)$$

$$\sigma_{ij}^t + \theta_i^t \geq (\hat{w}_{ij}^t - w_{ij}^t) y_j \quad \forall j \in S_i \quad (28)$$

$$\sigma_{ij}^t \geq 0 \quad \forall j \in S_i \quad (29)$$

$$\theta_i^t \geq 0 \quad (30)$$

6 Strong duality, along with the totally unimodular property, ensures that problems SPD_i^t
 7 (equations (27)-(30)) and SP_i^t (equations (24)-(26)), and consequently also the lhs of equation (14),
 8 are equivalent. Incorporating SPD_i^t in the equation (23), updates the robust formulation (equations
 9 (13), (15)-(21), (23)) to:

$$\max_{x,y,z,\sigma,\theta} \sum_{i \in I} c_i x_i \quad (31)$$

$$\sum_{j \in S_i} w_{ij}^t y_j^t + \sum_{j \in S_i} \sigma_{ij}^t + \Gamma_i^t \theta_i^t \leq \beta x_i \quad \forall i \in I, t \in T \quad (32)$$

$$\sigma_{ij}^t + \theta_i^t \geq (\hat{w}_{ij}^t - w_{ij}^t) y_j^t \quad \forall j \in S_i, i \in I, t \in T \quad (33)$$

$$\sum_{j \in J} y_j^t \leq q \quad \forall t \in T \quad (34)$$

$$\sum_{t \in T \setminus \{1\}} \sum_{j \in J} \sum_{k \in J} f_{jk}^t z_{jk}^t \leq B \quad (35)$$

$$\sum_{k \in J} z_{jk}^t = y_j^{t-1} \quad \forall j \in J, t \in T \setminus \{1\} \quad (36)$$

$$\sum_{j \in J} z_{jk}^t = y_k^t \quad \forall k \in J, t \in T \setminus \{1\} \quad (37)$$

$$x_i \in \{0, 1\} \quad \forall i \in I \quad (38)$$

$$y_j^t \in \{0, 1\} \quad \forall j \in J, t \in T \quad (39)$$

$$z_{jk}^t \in \{0, 1\} \quad \forall j, k \in J, t \in T \setminus \{1\} \quad (40)$$

$$\sigma_{ij}^t \geq 0 \quad \forall i \in I, j \in J, t \in T \quad (41)$$

$$\theta_i^t \geq 0 \quad \forall i \in I, t \in T \quad (42)$$

1 The above formulation is referred to as the robust maximum coverage facility location problem
 2 considering coverage reliability, abbreviated as MP-R. MP-R is a mixed-integer linear program
 3 and can be solved using open-source or commercially-available MIP solvers. For cases when $|T|$
 4 is large, the computational times using a MIP solver could be prohibitively large. The authors rec-
 5 ommend decomposition-based methodologies for such cases. For example, applying Lagrangian
 6 relaxation to equations (32) and (33) decomposes MP-R into four sub-problems, of which three
 7 can be trivially solved. The development of computationally-efficient heuristics is left as a future
 8 research endeavor.

9 COMPUTATIONAL ANALYSIS

10 This section first describes the experimental setting of the case study conducted in Portland,
 11 OR metropolitan area. Later, three types of analysis are conducted: computational performance,
 12 the evaluating the value of considering robustness and multiple periods using a Monte Carlo sim-
 13 ulation scheme, and finally, incorporating equity in decision-making.

14 The feasibility of using UAVs or drones for delivering defibrillators to demand points in
 15 the Portland, OR metropolitan area is evaluated here. The Portland Metro service area consists
 16 of 122 ZIP Code Tabulation Areas (ZCTA) which act as demand points, and 104 community cen-
 17 ters which act as potential launch sites as detailed in Chauhan et al. (22) and shown in Figure
 18 1. We evaluate drones against two service standards: the National Fire Protection Association's
 19 emergency response standard of providing coverage reliability of 90% within in a response time
 20 of 4 minutes (I), abbreviated as SS1; and, the 1997 US Emergency Medical Services Act service
 21 response standard of providing coverage reliability of 95% within a response time of 10 minutes
 22 (2), abbreviated as SS2. Two service standards are selected to evaluate the effect of increasing

1 response time on system performance and the value of data disaggregation using multiple time
 2 periods. All drones are equipped with an AED which weighs 1.5 kg each (38). A major factor
 3 leading to uncertainty in drone response times is wind speed and direction. The calculation of
 4 bounds of probability of failure (lower bound: p_{best} ; upper bound: p_{worst}) for delivering from
 5 a launch site to a demand point is carried out using procedure described in Algorithm 1, similar
 6 to (8), with sample size $n = 10,000$. The upper bound of probability of failure (p_{worst}) is con-
 7 sidered as worst-case probability ($\bar{p} + \hat{p}$). The nominal probability of failure (\bar{p}) is an average of
 8 bounds of variation weighted according to the distribution of wind directions.

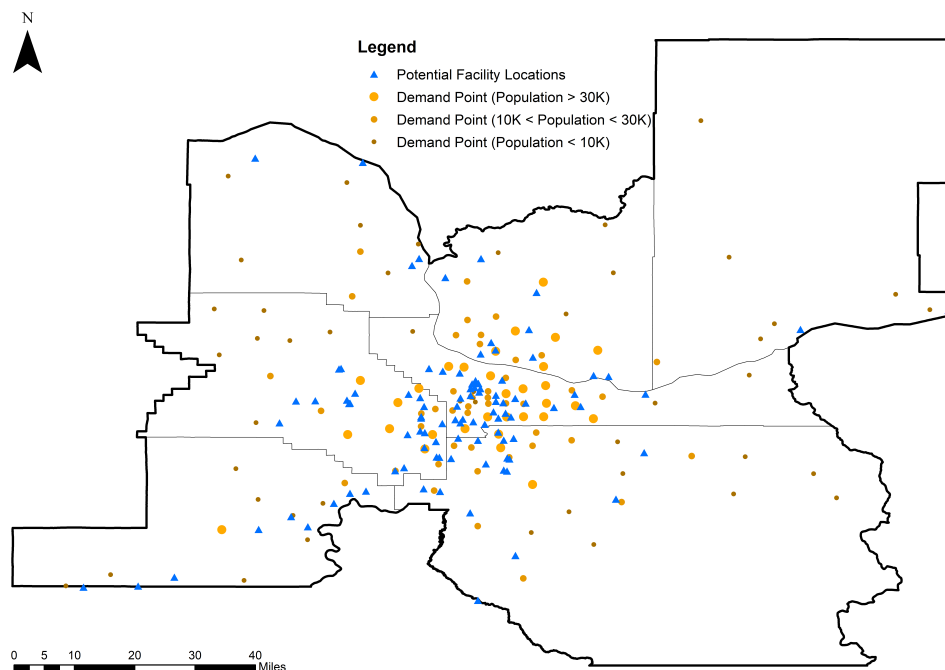


FIGURE 1: Locations of demand points and facility locations in Portland Metro Area

9 A demand point is considered accessible by a launch site if the following two conditions
 10 are met. First, the amount of battery expended to go to the demand point and come back is less
 11 than the total available battery in the nominal scenario (calculated using the formula provided in
 12 (39)). The total battery capacity of the drone is divided in two parts: total available battery and
 13 battery safety factor. As in Chauhan et al. (22), we assume that drones ignore obstacles in urban
 14 landscape and travel over Euclidean distances, and that the energy consumed in VTOL operations
 15 are accommodated in battery safety factor. Second, the time required to reach the demand point in
 16 the most favorable wind direction and speed is less than the provided response time. The coverage
 17 importance metric is dependent on the normalized population of the demand point. The ZCTA
 18 population estimates for the demand points were adopted from 2017 American Community Survey
 19 5-year estimates (40).

20 The summary of parameter specifications is provided below (8, 39).

- 21 • Maximum available battery: 777 Wh
 22 • Battery Safety Factor: 20% of maximum available battery (Total available battery =
 23 maximum available battery – battery safety factor = 621.6 Wh)

- 1 • Sum of drone tare and battery mass: 10.1 kg
2 • Lift-to-drag ratio: 2.8445
3 • Total power transfer efficiency: 0.66
4 • Nominal travel speed of drone: 20 meters per second (mps)
5 • Maximum number of drones serving demand point i in time period t that can achieve
6 worst-case probability of failure (Γ_i^t): 1
7 • $c_i = \text{Normalized population of demand point } i = \left\lceil \frac{100 \times \text{population of demand point } i}{\text{maximum population of demand points}} \right\rceil$
8 • Wind speed and direction distributions (see Figure 2) are available openly at
9 <https://github.com/drc1807/RMP-MCFLP-CR>
10 • Maximum possible wind speed: 68 miles per hour (30.3987 mps)
11 • The planning period is one year. In Portland, the wind direction is primarily in the NW
12 direction in the summer months (April through September). Whereas, in winter months
13 (October through March), the wind primarily flows in the ESE direction (see Figure 2).
14 We investigate the value of using a multi-period formulation with $T = \{\text{Summer, Winter}\}$
15 over a single-period formulation with $T = \{\text{Whole Year}\}$.
16 where $\lceil u \rceil$ represents the ceiling function, i.e. the least integer greater than or equal to u . The
17 model coverage (in %) is given as:

$$\text{Model Coverage} = \frac{\text{Objective Value of Model}}{\sum_{i \in I} c_i} \times 100 \quad (43)$$

Algorithm 1 Calculating bounds of probability of failure

Input sample size n , wind speed and direction distributions for each time period $t \in T$, maximum possible wind speed (v_{wind_max}), probability distribution of wind directions, response time (τ), drone travel speed (v_{drone}), and distance ($dist_act$) and delivery angle from facility j to demand point i .

Calculate $wt[i, j, t]$ which is the probability that the wind direction is not aligned with the delivery direction (i.e. difference is greater than 90°) from facility j to demand point i in time period t using the input information.

for $t \in T$ **do**

 Generate $windspeeds[t]$, an array of size n , following a lognormal distribution with given input parameters and a maximum value of v_{wind_max} .

$dist_best = (v_{drone} + windspeeds[t]) \cdot \tau$

$dist_worst = (v_{drone} - windspeeds[t]) \cdot \tau$

for $i \in I$ **do**

for $j \in J$ **do**

$p_best[i, j, t] = \max\{\text{length}(\text{where}(dist_best < dist_act[i, j])), 1\}/n$

$p_worst[i, j, t] = \max\{\text{length}(\text{where}(dist_worst < dist_act[i, j])), 1\}/n$

$p_nominal[i, j, t] = (1 - wt[i, j, t]) \cdot p_best[i, j, t] + wt[i, j, t] \cdot p_worst[i, j, t]$

end for

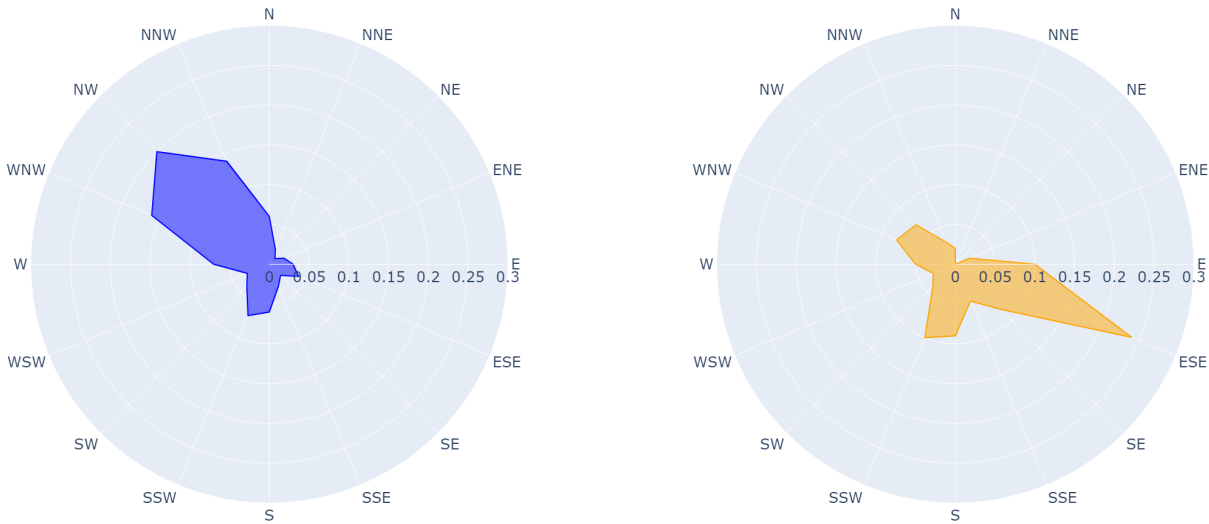
end for

end for

- 18 The cost of shifting a facility located at $j \in J$ in time period $(t - 1)$ to a location $k \in J, k \neq j$

1 in time period t is considered to be 1, and 0, if the location does not change. Alternatively put,
 2 $f_{jj}^t = 0 \forall j \in J, t \in T \setminus \{1\}$, and 1, otherwise. This limits the total number of facility location shifts
 3 to the facility shifting cost budget B . The default value of B used here is $\lfloor 0.35q \rfloor$, where q is the
 4 maximum number of drone launch sites that can be opened.

5 The experiments are performed on four models: MP-R, MP-D, MP-R with $T = \{\text{Whole Year}\}$
 6 (abbreviated as SP-R), and MP-D with $T = \{\text{Whole Year}\}$ (abbreviated as SP-D) considering a
 7 planning period of a whole year. Models are solved using Gurobi (41) in Python interface on a
 8 Windows 10 desktop with Intel i7-7700K processor and CPU specifications of 3.6 GHz, 4 cores,
 9 8 logical processors, and 32 GB of RAM. Experiments to evaluate the computational efficiency
 10 with an increasing number of drone launch sites (q) are conducted, followed by the evaluation
 11 of the value added by robustness and granularity of information (through multiple time periods).
 12 Additionally, the effect of adding equity in decision-making is explored.



(a) Summer

(b) Winter

FIGURE 2: Wind direction distribution in Portland, OR

13 Computational Efficiency

14 Prohibitive computational times can often be a barrier to model adoption in real life. In our case,
 15 the planning period is fairly large (a whole year), and therefore, no computational time limit was
 16 adopted for Gurobi. All the four models, for both service standards and given default values of
 17 parameters, converged in less than 2 hours for a range of q values, indicating that the development
 18 of time-efficient heuristics was not required. The model coverage values with their computational
 19 times are provided in Table 1.

20 The effect of adding additional time periods is found to be more profound than the effect of
 21 adding robustness to the formulation. On average, for SS1, adding robustness increases computa-
 22 tional time by 5.2 times, whereas adding additional time-period increases computational times by
 23 37.0 times. For SS2, these values are 24.5 times and 49.5 times, respectively. The primary reason
 24 behind this is the number of constraints added to the model. A multi-period formulation requires
 25 the facility transfer variables z which adds $2 \cdot |J| \cdot |T \setminus \{1\}|$ facility matching equality constraints

1 along with a facility relocation budget constraint. Additionally, $|T| - 1$ simultaneous coverage re-
 2 liability constraints are also added which further deteriorates computational performance. On the
 3 other hand, adding robustness adds more variables and constraints to the model, but the constraints
 4 are computationally simpler. The accessibility matrix A is more sparse for the SS1 models than
 5 SS2 models, which leads to better computational performance.

6 The addition of multiple periods to the formulation decreases the model coverage by a
 7 little amount (0.8% on average). This is because the satisfaction of multiple coverage reliability
 8 constraints is required for demand point coverage. As expected, adding robustness decreases the
 9 model coverage by a significant amount (4.9% on average) as a consequence of accounting for
 10 worst-case scenarios.

TABLE 1: Computational Efficiency

Service Standard	q	Model Coverage (%)				Computational Time (sec)			
		MP-R	MP-D	SP-R	SP-D	MP-R	MP-D	SP-R	SP-D
SS1	3	12.57	15.76	12.9	15.76	32	6	2	1
	6	24.37	27.41	24.64	28.19	109	15	3	1
	9	33.52	37.93	34.62	38.8	416	17	3	1
	12	41.9	47.02	42.64	48.36	444	33	2	1
	15	49.28	53.9	49.37	55.6	44	23	2	1
	20	55.45	62.31	55.21	62.99	49	8	2	1
	25	59.92	67.19	59.09	67.4	44	4	2	1
	30	62.28	68.36	62.1	68.56	5	4	1	1
35	62.28	68.5	62.28	68.71	2	1	1	1	
SS2	3	35.37	44.85	39.09	46.31	5736	152	38	2
	6	62.69	69.99	64.75	72.53	3937	152	64	1
	9	75.8	82.18	77.26	83.02	1342	26	44	1
	12	82.6	86.23	83.28	87.84	569	40	67	1
	15	87.01	89.6	87.19	90.91	694	44	32	1
	20	90.73	93.38	90.88	93.95	274	108	20	1
	25	92.58	94.73	92.76	95.68	45	48	9	1
	30	93.21	95.23	93.36	96.39	31	2	14	1
35	93.38	95.29	93.53	96.63	2	1	1	1	

Note:

SS1 is providing 90% coverage reliability in a response time of 4 minutes

SS2 is providing 95% coverage reliability in a response time of 10 minutes

11 Value of developing multi-period formulation and adding robustness

12 The value of using more information (through adding robustness and multiple time periods) in
 13 a model is evaluated in this section utilizing a Monte-Carlo simulation-based (MCS) framework.
 14 Generally, adding robustness to a formulation reduces the model coverage but should provide for
 15 better real-life performance, thereby reducing the gap between what is expected (model coverage)
 16 and what happens (simulated coverage). Similarly, having potentially different facility location
 17 layouts in different time periods should boost simulated coverage.

18 An MCS framework is proposed to quantify the value of using additional information. In
 19 an MCS scenario s , the time period is t^s , and $n = 1000$ values of wind directions and speeds are

1 randomly generated. In our case, an MCS scenario s can be thought of as a day of the year, and n
 2 is the number of wind speed and direction observations made throughout the day. Therefore, for
 3 multi-period formulations, $t^s = \text{'Summer'}$ with probability $183/365$ and $t^s = \text{'Winter'}$ with proba-
 4 bility $182/365$. For single-period formulations, $t^s = \text{'Whole Year'}$ with probability 1. Depending on
 5 the value of t^s , the wind speeds are generated as in Algorithm 1 and wind directions are chosen as
 6 per the distributions of the time period. These angles and speeds are combined with the originally
 7 projected delivery angles and nominal drone delivery speed to find effective drone speed. The ef-
 8 fective drone speeds are then utilized to determine the realizations of the probability of failure for
 9 the scenarios (\tilde{p}^s).

10 The solutions obtained from the robust and the deterministic formulations for the variable
 11 y are denoted by y^* . The new values for the variable x (denoted by \tilde{x}) and the actual coverage are
 12 calculated using y^* and \tilde{p}^s . For multi-period formulation, the facility location layout is determined
 13 by the simulation time period t^s . A total of 100 MCS scenarios are evaluated and the algorithm for
 14 the described MCS is detailed in Algorithm 2.

Algorithm 2 Monte Carlo simulation for evaluating coverage

Input number of MCS scenarios (MCS_s), number of wind speed and direction observations per
 scenario (n), probability distribution of time periods $t \in T$ (π), other model input parameters

Solve the model and determine y^* , the optimum values of decision variable y

Determine J_i , the set of open and accessible facilities for each demand point $i \in I$

$s = 1$

$simulated_coverage = zeros(MCS_s)$

while $s \leq MCS_s$ **do**

 Randomly select simulation time period t^s , such that $t^s = t$ with probability π_t

 Generate $windspeeds[t^s]$, an array of n elements, as in Algorithm 1

 Generate $windangles[t^s]$, an array of n elements, based on the probability distribution in time
 period t^s

 Determine effective delivery angles and effective drone speeds using vector algebra.

 For each i, j combination, calculate $dist_cov_{ij}^s$, an array of length n describing distances cov-
 ered by drones using effective delivery angles and effective drone speeds.

 For each i, j combination, calculate $\tilde{p}_{ij}^s = length(when(dist_cov_{ij}^s < dist_act[i, j]))/n$

$\tilde{w}^s = \log(\tilde{p}^s)$

$\tilde{x}^s = zeros(length(I))$

for $i \in I$ **do**

if $\sum_{j \in J_i} \tilde{w}_{ij}^s y_j^* \leq \beta$ **then**

$\tilde{x}_i^s = 1$

end if

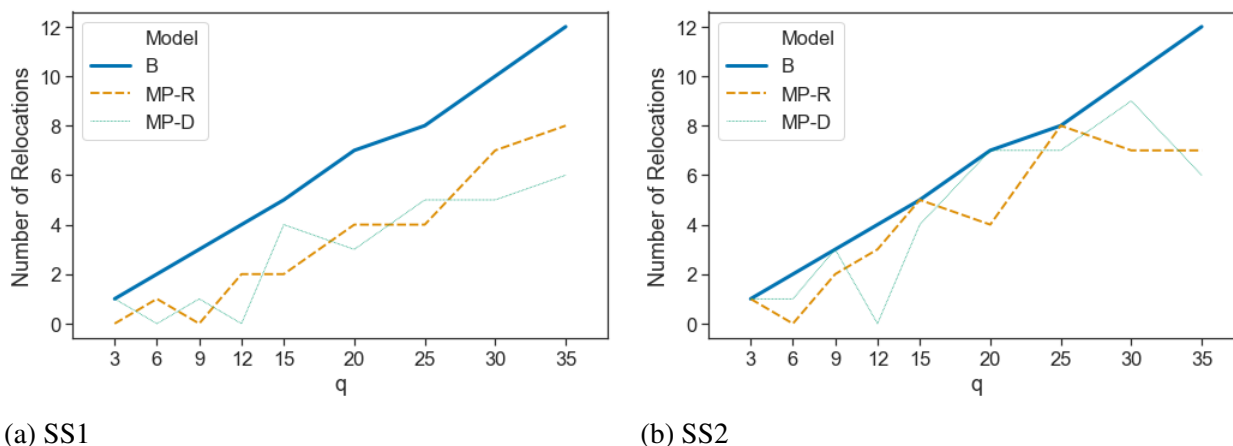
end for

$simulated_coverage[s] = \frac{\sum_{i \in I} c_i \tilde{x}_i^s}{\sum_{i \in I} c_i} \times 100$

$s + = 1$

end while

1 The simulated coverage values for all four models with default values are presented in
 2 Table 2. For SS1 (providing 90% coverage reliability in 4 minutes), extending to multi-period
 3 formulation improves average simulated coverage by 0.29 times on average for robust models, and
 4 by 0.41 times on average for deterministic models. Whereas for SS2 (providing 95% coverage
 5 reliability in 10 minutes), the improvements in average simulated coverage are by 0.02 times for
 6 robust models, and by 0.24 times for deterministic models. The improvements are higher when
 7 the response time is short because the importance of choosing the right set of facility locations
 8 increases. An explanatory factor would be that multi-period formulation allows for more flexibility
 9 by allowing changing facility locations for different periods. The extent of facility relocation is
 10 depicted in Figure 3. The results reveal that at least 40% of the relocation budget is used when
 11 15 or more facilities are opened. To further investigate the role of facility relocation, consider the
 12 visualization of facility location by season for MP-R SS2 model with $q = 15$, as an example, in
 13 Figure 4. Based on the wind patterns in Portland (see Figure 2), we expect the facilities in the
 14 summer season to provide better coverage reliability to demand locations in the west and/or north
 15 directions of them. As a result, the facility locations should be skewed a little bit towards the eastern
 16 and/or southern region of the operational area. Similarly, the locations in the winter season should
 17 be skewed a little bit towards the western and/or northern region. For our considered example,
 18 we indeed note that the centroid of facility locations opened in summer only is to the east of the
 19 centroid of facility locations opened in winter only, which is in agreement with our hypothesis.



(a) SS1

(b) SS2

FIGURE 3: Facility relocations in multi-period formulation (B represents maximum allowable facility relocations)

TABLE 2: Value of extending to multi-period formulation and adding robustness

Model	q	SS1				SS2			
		Model Cov. (%)	Simulated Cov. (%) Min	Ave	Max	Model Cov. (%)	Simulated Cov. (%) Min	Ave	Max
MP-R	3	12.57	5.96	9.28	11.11	35.37	21.42	26.47	32.6
	6	24.37	13.89	16.59	19.55	62.69	36.59	46.01	56.38
	9	33.52	16.3	22.3	26.97	75.8	56.08	63.44	67.07
	12	41.9	24.52	29.96	35.67	82.6	66.18	72.25	79.38
	15	49.28	32.39	37.82	44.85	87.01	72.77	75.36	79.02
	20	55.45	35.58	45.26	53.67	90.73	72.62	78.47	85.97
	25	59.92	43	48.71	54.68	92.58	77.26	81.81	89.09
	30	62.28	48.99	52.58	56.05	93.21	77.98	83.21	88.86
	35	62.28	50.92	53.26	56.53	93.38	86.41	90.91	92.7
MP-D	3	15.76	5.81	8.56	10.25	44.85	23.27	24.75	28.07
	6	27.41	7.9	14.03	19.43	69.99	14.96	31.01	45.74
	9	37.93	14.66	21.79	28.22	82.18	45.05	51.95	60.25
	12	47.02	19.22	27.83	35.43	86.23	47.44	55.65	66.15
	15	53.9	24.76	32.04	39.81	89.6	41.87	51.32	64.99
	20	62.31	25.3	35.16	44.31	93.38	50.48	60.82	71.48
	25	67.19	34.45	40.98	47.5	94.73	68.33	74.49	78.55
	30	68.36	37.22	46.33	55.69	95.23	67.04	77.36	84.77
	35	68.5	40.88	48.01	58.19	95.29	77.83	83.27	90.67
SP-R	3	12.9	1.1	3.54	7.87	39.09	19.34	28.89	32.93
	6	24.64	10.37	11.96	18.06	64.75	36.92	42.25	52.18
	9	34.62	14.36	17.66	24.67	77.26	52.89	62.33	68.47
	12	42.64	23.81	28.73	34.92	83.28	58.88	65.28	74.91
	15	49.37	26.91	34.26	43	87.19	68.98	77.46	83.37
	20	55.21	29.05	40.63	50.63	90.88	70.98	78.71	84.86
	25	59.09	40.05	45.95	53.93	92.76	77.18	80.4	82.93
	30	62.1	42.01	50.33	57.33	93.36	76.28	81.65	89.06
	35	62.28	46.84	52.95	58.94	93.53	87.34	89.74	91.87
SP-D	3	15.76	3.93	4.53	6.23	46.31	18.98	22.57	26.82
	6	28.19	3.72	6.44	9.92	72.53	22.56	29.9	37.4
	9	38.8	7	11.68	16.78	83.02	32.06	41.54	47.94
	12	48.36	14.75	22.49	31.35	87.84	30.78	38.76	44.73
	15	55.6	19.19	25.42	32.75	90.91	29.14	38.72	46.28
	20	62.99	21.22	29.61	38.53	93.95	30.13	40.03	48.81
	25	67.4	32.03	40.82	47.94	95.68	54.02	57.29	63.29
	30	68.56	33.97	42.47	50.83	96.39	61.29	67.56	74.76
	35	68.71	39.6	48.4	54.08	96.63	72.82	77.38	80.39

Note:

Cov. = Coverage

SS1 is providing 90% coverage reliability in a response time of 4 minutes

SS2 is providing 95% coverage reliability in a response time of 10 minutes

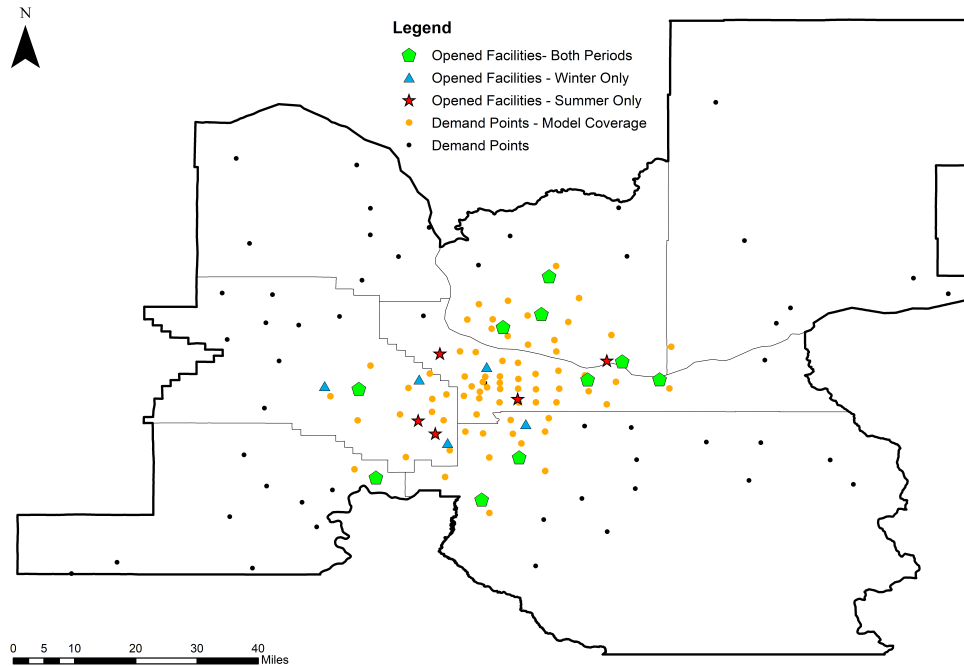


FIGURE 4: Facility relocation and model coverage for MP-R (SS2; $q = 15$)

1 For SS1, the improvements in average simulated coverage achieved by adding robustness
 2 to multi-period and single-period formulations are by 0.14 times and 0.28 times, respectively. For
 3 SS2, the improvements in average simulated coverage are by 0.23 times and 0.51 times for multi-
 4 period and single-period formulations, respectively. The improvement by adding robustness to a
 5 multi-period formulation is lower as more detailed information has been accounted which leads
 6 to lower variability in data in each time period. Similarly, the variability in distance traveled by
 7 drone would increase with an increase in response time which leads to greater variability in failure
 8 probabilities. Therefore, the benefit obtained by adding robustness is greater when response times
 9 are longer. Overall, going from a single-period deterministic (SP-D) formulation to a multi-period
 10 robust (MP-R) formulation leads to an average simulated coverage improvement of 0.60 times
 11 and 0.54 times for SS1 and SS2, respectively. Figures 5 and 6 show model solution and an MCS
 12 simulation solution (having simulated coverage close to the average value) for SP-D and MP-R,
 13 respectively, for SS2 and $q = 15$. Accommodating uncertainty in decision-making leads to the
 14 consolidation of facilities towards the central core of the Portland Metro Area. Shorter travel
 15 distances lead to better coverage reliability in in the MP-R model.

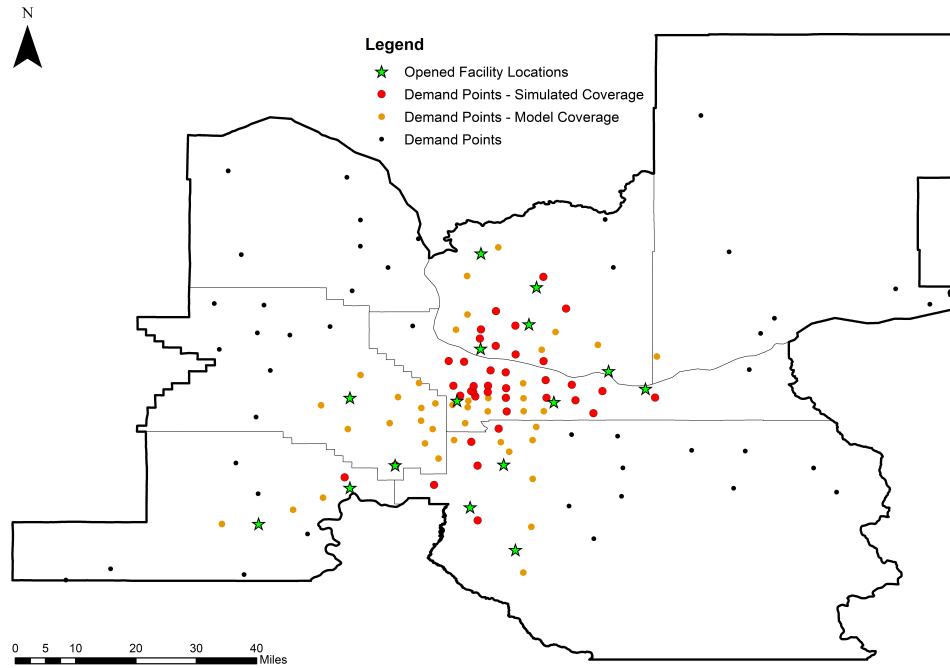


FIGURE 5: Opened Facility Locations and Demand Point Coverage for SP-D (SS2; $q = 15$)

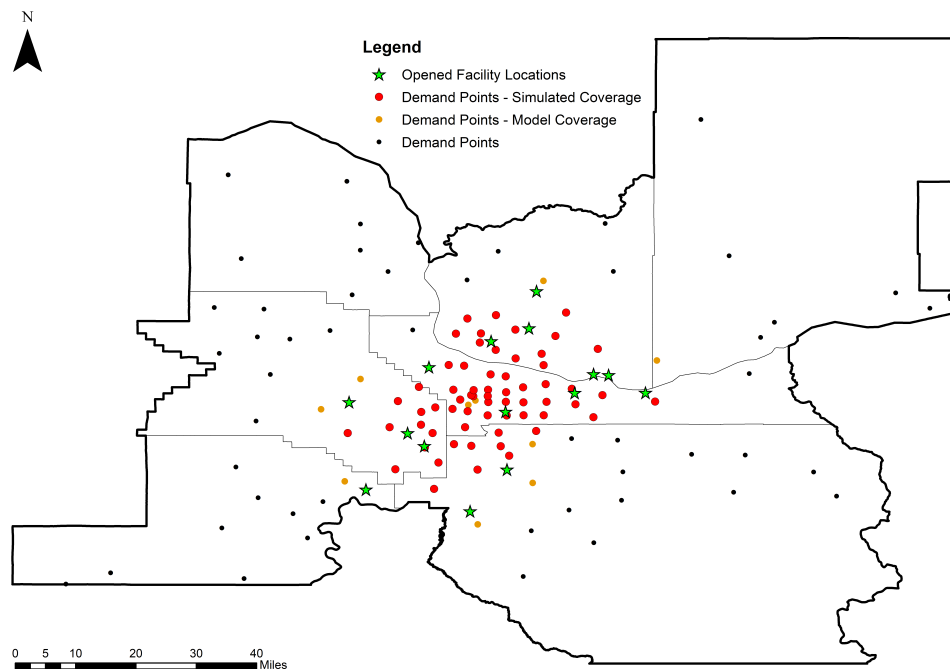


FIGURE 6: Opened Facility Locations and Demand Point Coverage for MP-R (SS2; $q = 15$; $\Gamma_i^r = 1$)

1 Figure 7 shows the ratio of average simulated coverage to the model coverage (ASC-to-
 2 MC). The closer the values to 1 the better, as it indicates that the expected performance is close to
 3 real-life simulated scenarios. Accounting for robustness and/or extending to multi-period formu-
 4 lation leads to better outcomes on this metric. The ratio has a generally positive correlation with
 5 increasing values of q . This is expected, as with more opened facilities, the access to a demand
 6 point improves, and therefore, the coverage reliability also improves.

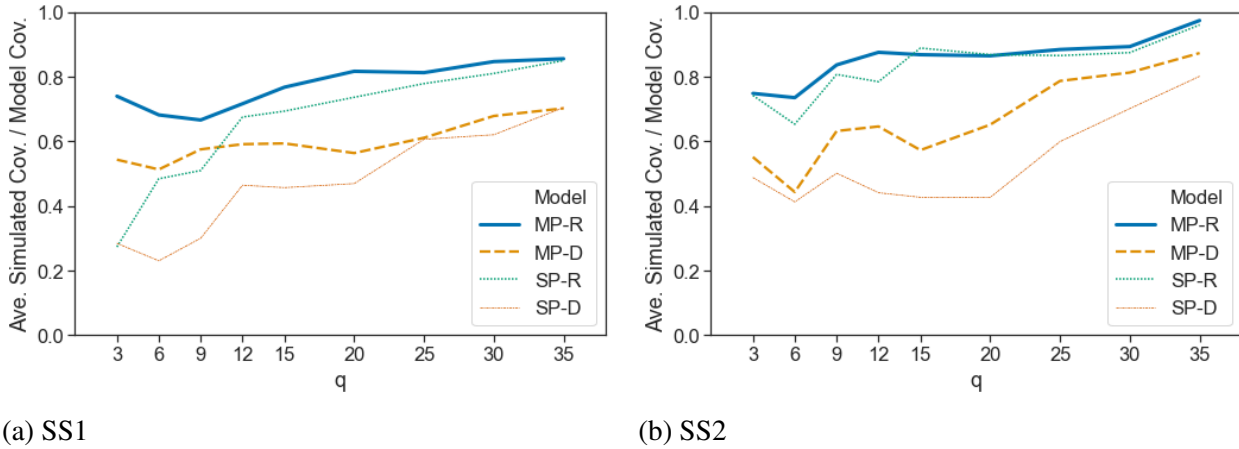


FIGURE 7: Ratio of average simulated coverage to model coverage

7 Table 3 shows the sensitivity of increasing conservatism on the coverage. For SS1, in-
 8 creasing robustness by increasing Γ_i^r from 1 to 2 does not change the average simulated coverage
 9 much (-0.01 times). For SS2, this results in slightly better average simulated coverage (0.04 times).
 10 Computational times on the other hand typically increased with an increase in the budget of ro-
 11 bustness. However, all models still converged in 8 hours, which is still not much considering a
 12 planning period of one year. Figure 8 shows the variation of computational times with the budget
 13 of robustness.

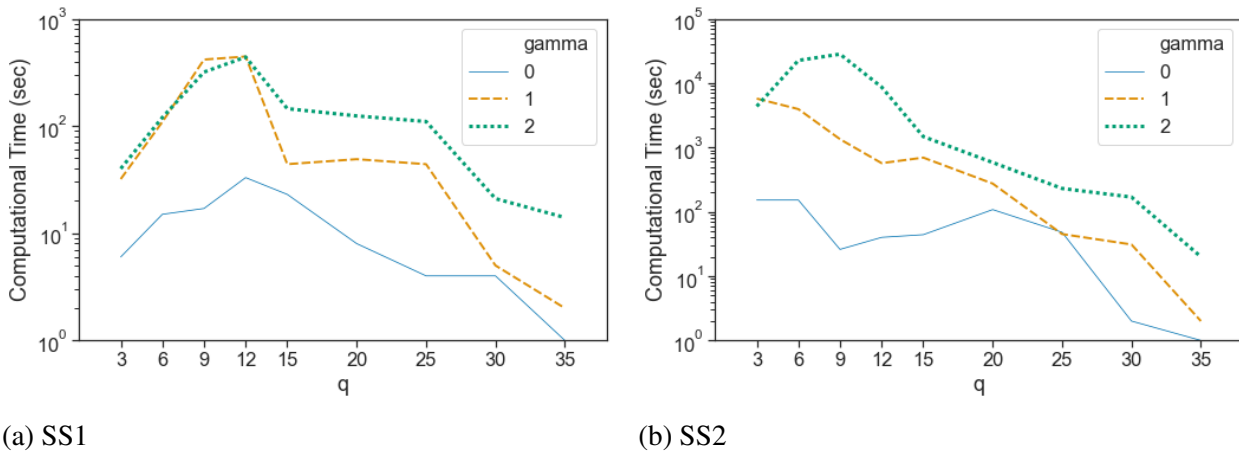


FIGURE 8: Computational times for varying values of Γ_i^r in multi-period formulation

TABLE 3: Sensitivity to increasing conservatism in decision-making for multi-period formulation

Γ_i^r	q	SS1				SS2			
		Model Cov. (%)	Simulated Cov. (%)			Model Cov. (%)	Simulated Cov. (%)		
			Min	Ave	Max		Min	Ave	Max
0	3	15.76	5.81	8.56	10.25	44.85	23.27	24.75	28.07
	6	27.41	7.90	14.03	19.43	69.99	14.96	31.01	45.74
	9	37.93	14.66	21.79	28.22	82.18	45.05	51.95	60.25
	12	47.02	19.22	27.83	35.43	86.23	47.44	55.65	66.15
	15	53.90	24.76	32.04	39.81	89.60	41.87	51.32	64.99
	20	62.31	25.30	35.16	44.31	93.38	50.48	60.82	71.48
	25	67.19	34.45	40.98	47.50	94.73	68.33	74.49	78.55
	30	68.36	37.22	46.33	55.69	95.23	67.04	77.36	84.77
	35	68.50	40.88	48.01	58.19	95.29	77.83	83.27	90.67
1	3	12.57	5.96	9.28	11.11	35.37	21.42	26.47	32.60
	6	24.37	13.89	16.59	19.55	62.69	36.59	46.01	56.38
	9	33.52	16.30	22.30	26.97	75.80	56.08	63.44	67.07
	12	41.90	24.52	29.96	35.67	82.60	66.18	72.25	79.38
	15	49.28	32.39	37.82	44.85	87.01	72.77	75.36	79.02
	20	55.45	35.58	45.26	53.67	90.73	72.62	78.47	85.97
	25	59.92	43.00	48.71	54.68	92.58	77.26	81.81	89.09
	30	62.28	48.99	52.58	56.05	93.21	77.98	83.21	88.86
	35	62.28	50.92	53.26	56.53	93.38	86.41	90.91	92.70
2	3	12.57	5.96	9.28	11.11	33.85	23.96	25.98	31.62
	6	22.35	8.61	15.13	20.89	59.92	41.21	48.19	55.27
	9	30.99	16.12	21.36	25.74	73.60	57.54	63.83	69.49
	12	39.18	26.88	29.39	32.48	80.51	73.48	76.81	79.35
	15	45.65	32.99	38.29	45.11	85.40	75.27	79.28	82.39
	20	52.23	39.72	46.24	52.62	89.81	81.85	85.18	87.84
	25	56.59	43.12	49.16	53.87	92.01	82.54	86.01	86.86
	30	60.07	48.72	51.70	55.13	93.00	85.04	88.45	91.00
	35	61.92	51.37	54.68	58.46	93.38	87.19	89.53	90.20

1 Significant improvements in range of variation in simulated coverage as well as in the ratio
2 ASC-to-MC were found, especially for larger values of q . These results are as expected as ac-
3 counting for more amount of uncertainty should lead to reduced model coverage (due to increased
4 conservatism) and less variability in results (due to reduced probability of constraint violation).
5 Therefore, finding a trade-off by changing the budget of robustness (Γ_i^r) can help improve the
6 simulated coverage values, and reduce its gap from the model coverage. For example, Figure 9
7 shows variation in model and average simulated coverage with increasing value of Γ_i^r for MP-R
8 SS1 model with $q = 35$. It can be noticed that the gap between the model and average simulated
9 coverage is the minimum when $\Gamma_i^r = 4$.

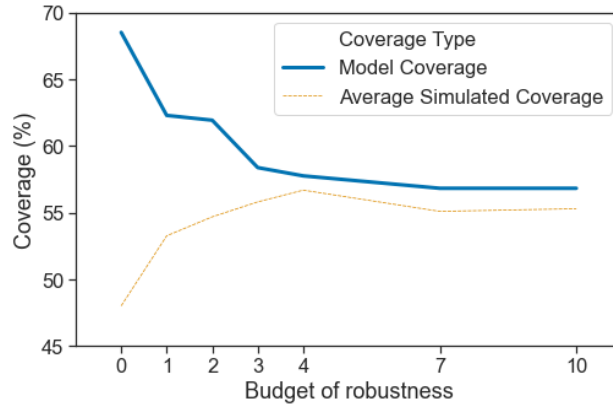


FIGURE 9: Model and Average Simulated Coverage with increasing values of budget of robustness Γ_i^r (MP-R SS1 with $q = 35$)

1 Figure 10 shows model solution and an MCS simulation solution (having simulated cover-
 2 age close to the average value) for MP-R with $\Gamma_i^r = 2$ (SS2 and $q = 15$). Increasing conservatism
 3 further consolidates facilities around the central core compared to the case when $\Gamma_i^r = 1$ in MP-R,
 4 leading to better outcomes in terms of simulated coverage.

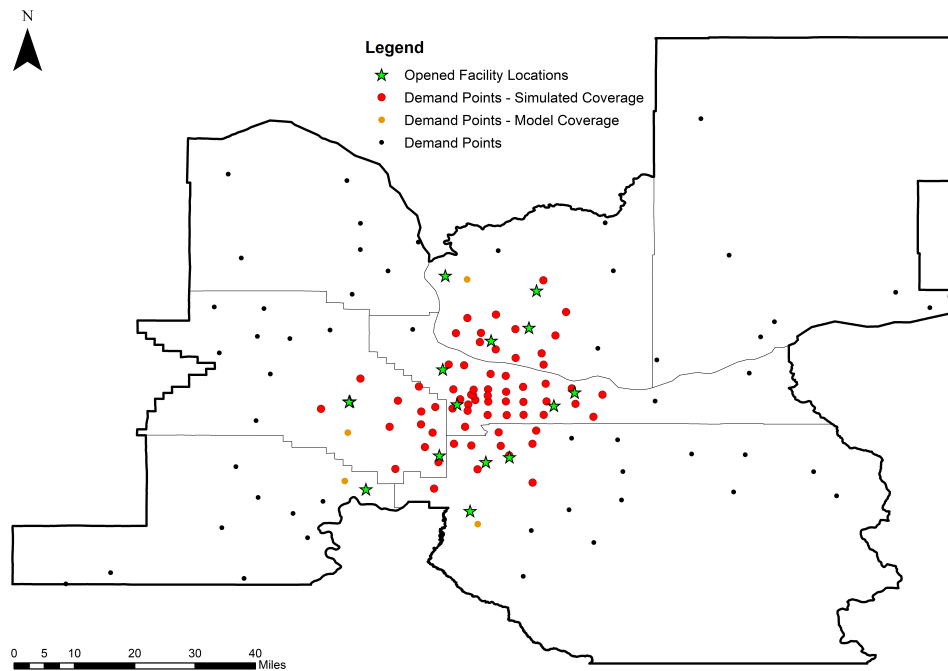


FIGURE 10: Opened Facility Locations and Demand Point Coverage for MP-R (SS2; $q = 15$; $\Gamma_i^r = 2$)

5 **Incorporating equity in decision-making**

6 For the previous sections, the coverage importance was just based on the normalized population
 7 of the demand points. However, it is possible to incorporate equity-related weights to determine

1 coverage importance. For our case study, it can be considered that the facility locations that are not
 2 opened still have a defibrillator available onsite, just that they can not be transported. Therefore,
 3 distance to the nearest potential facility location could be considered as a metric of equity, as in
 4 (42). The larger the minimum distance to a potential facility location from a demand point, the less
 5 equitable it is, and the more coverage importance it should get. The normalized inequity metric is
 6 calculated as:

- 7 • Distance to closest possible drone launch site from demand point i : $mindist(i)$
- 8 • Normalized inequity metric of demand point $i = \left[\frac{100 \times mindist(i)}{\text{maximum value of } mindist(i)} \right]$

9 For calculating the coverage importance metric, 50% weightage is assumed for both, the
 10 normalized population parameter, and the normalized inequity metric. Other parameters are set
 11 to their default values. The summary of results is shown in Figure 11. The simulated coverage
 12 values when equity is included are much lower than the values when equity is not included. When
 13 equity is included, the demand points far away from potential facility locations are given more
 14 importance, but, most of them can not even be accessed in the target response times (i.e. $|S_i|$ is
 15 a very small number). The spatial distribution of facilities and the demand coverage when equity
 16 is included is shown in figure 12 for the MP-R SS2 model with $q = 15$. It can be noticed that
 17 the figures 6 and 12 are very similar, covering almost the same demand points and most facilities
 18 opened at the same spot. A primary reason for this is the distribution of facility locations and
 19 demand points. The demand points outside the more densely populated central core are located
 20 too far away from the potential facility locations. For the response times used in our case study,
 21 it does not make a practical difference if equity is included or not. However, for longer response
 22 times, equity inclusion could be beneficial (longer response times lead to larger values of $|S_i|$,
 23 which make it easier to meet service reliability target for all demand points).

24 Aringhieri et al. (17) state that equity is still one of the most challenging concerns for
 25 emergency medical services. More comprehensive methodologies that explicitly address equity
 26 concerns should be explored. Previous works in facility location have addressed equity by using
 27 metrics based on distance, exclusion, and conditional value-at-risk in model formulation (43).

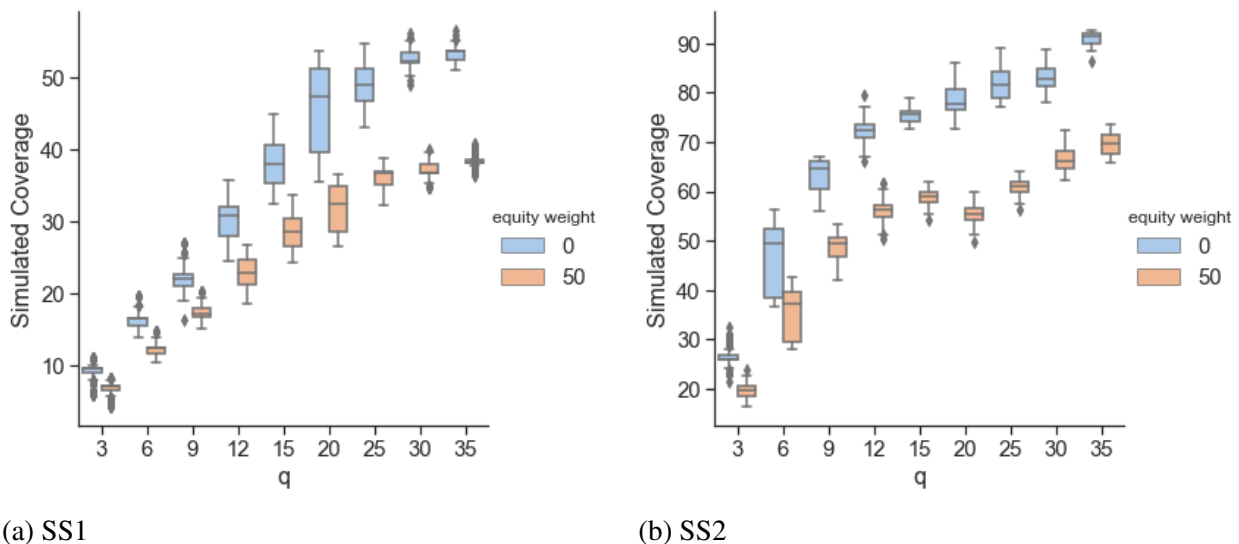


FIGURE 11: Effect of incorporating equity on simulated coverage

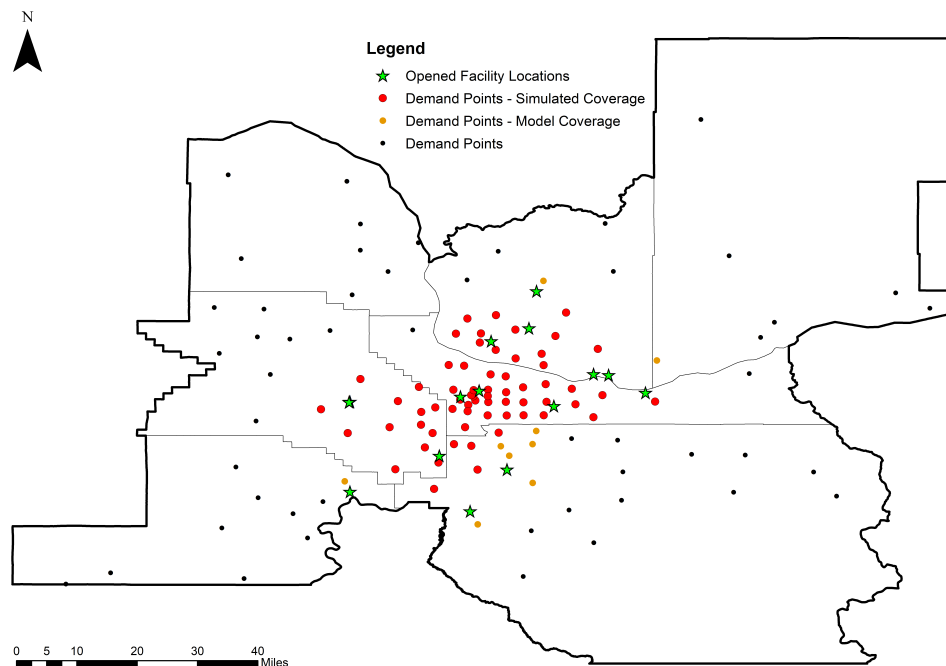


FIGURE 12: Opened Facility Locations and Demand Point Coverage for MP-R with equity inclusion (SS2; $q = 15$; $\Gamma_i^t = 1$)

1 CONCLUSION

2 This paper proposes a robust multi-period maximum covering facility location problem
 3 with coverage reliability (MP-R). MP-R is a generalized variant of the robust uncertain set covering
 4 the problem proposed by Lutter et al. (2). The problem incorporates uncertainty in travel times
 5 via chance constraints and uses robust optimization using polyhedral uncertainty sets to tackle
 6 uncertainty. More conservative solutions can be obtained by increasing the value of parameter Γ_i^t .

7 A case study of the use of unmanned aerial vehicles (UAVs) or drones to deliver defibrilla-
 8 tors in the Portland Metro Area is proposed. The uncertainty in drone travel times is a product of
 9 natural variability in wind speeds and directions. In Portland, the wind characteristics (speed and
 10 direction) change drastically between the summer months (April to September) and winter months
 11 (October to March). Therefore, multiple periods are thought of as a discretization of recurring
 12 planning intervals (here, one whole year). We evaluate the effect of extending from a single period
 13 formulation (a whole year) to a multi-period formulation (two different time periods: summer and
 14 winter).

15 The value of adding robustness and extending to a multi-period formulation was evalu-
 16 ated utilizing a novel Monte-Carlo simulation scheme. The results highlighted that utilizing a
 17 multi-period formulation was particularly beneficial when response time thresholds were short or
 18 when uncertainty is not accounted for in the model. On the other hand, adding robustness to the
 19 deterministic models was more beneficial for single-period formulations or when response time
 20 thresholds were longer. Combining these different strengths led to an increase in average simu-
 21 lated coverage of MP-R by 57% compared to the deterministic single-period formulation (SP-D).
 22 Geographically, accounting for uncertainty (in MP-R) consolidates the facility locations towards
 23 the dense central core of the metro area compared to more spread out locations in SP-D. A more

1 compact facility layout in MP-R improves the level of service in the central core of the metro area
2 leading to superior simulated coverage.

3 For the MP-R model, a sensitivity analysis on the facility relocation cost budget showed
4 very minor changes in model coverage as well as simulated coverage values. This implies that
5 simply providing the model with more detailed information by discretizing over the planning pe-
6 riod (even when facility relocation is not allowed) is helpful rather than providing the average
7 information of the planning period. From our case study, when the response times are shorter, we
8 recommend that an existing SP-D model should be extended to MP-R (i.e., incorporating uncer-
9 tainty and discretizing to multiple periods). When the response times are longer, only incorporating
10 uncertainty in the SP-D model is sufficient and multiple periods are not necessary.

11 The presented formulation can be used to analyze equity gaps and the need for additional
12 resources. Analysis of distance-based equity inclusion in the objective yielded poorer coverage
13 values. Equity inclusion increases the coverage importance of demand points further away from
14 potential drone launch sites, but response times used in our study were too short for these points
15 to be covered reliably. Geographically, equity inclusion did not affect the facility locations and
16 demand point coverage significantly. However, for longer response times than used in this study,
17 equity inclusion could be beneficial.

18 Even with the MP-R model providing the best performance, a significant gap exists between
19 model coverage and the simulated coverage values. A major contributing factor is the assumption
20 of independence among the failure probabilities. While some of the gap can be addressed by ad-
21 justing the budget of uncertainty and increasing the number of opened facilities, there is still a
22 need to account for correlation in failure probabilities. Additionally, the study assumed that all
23 the accessible open facilities respond to the demand while not considering the possible unavail-
24 ability of a drone at a located launch site. Future studies should also focus on including capacity
25 considerations at located launch sites.

26 **AUTHOR CONTRIBUTIONS**

27 The authors confirm contribution to the paper as follows: study conception and design: all
28 authors; data collection: D.R. Chauhan; analysis and interpretation of results: D.R. Chauhan, A.
29 Unnikrishnan, M. Figliozzi; draft manuscript preparation: all authors. All authors reviewed the
30 results and approved the final version of the manuscript. The authors do not have any conflicts of
31 interest to declare.

32 **ACKNOWLEDGMENTS**

33 This work was supported by the Freight Mobility Research Institute, the Center for Ad-
34 vanced Multimodal Mobility Solutions and Education, and the National Science Foundation under
35 grants CMMI-1562109/1562291: Collaborative Research: Non-Additive Network Routing and
36 Assignment Models, CMMI-1636154: Optimal Control of a Swarm of Unmanned Aerial Vehicles
37 for Traffic Flow Monitoring in Post-disaster Conditions, and CMMI 1826320/1826337: Collabo-
38 rative Research: Real-Time Stochastic Matching Models for Freight Electronic Marketplace.

1 REFERENCES

- 2 1. *NFPA 1710: Standard for the Organization and Deployment of Fire Suppression Operations, Emergency Medical Operations, and Special Operations to the Public by Career Fire Departments*. National Fire Protection Agency, 2020.
- 3
- 4
- 5 2. Lutter, P., D. Degel, C. Büsing, A. M. Koster, and B. Werners, Improved handling of
6 uncertainty and robustness in set covering problems. *European Journal of Operational*
7 *Research*, Vol. 263, No. 1, 2017, pp. 35–49.
- 8 3. Budge, S., A. Ingolfsson, and D. Zerom, Empirical analysis of ambulance travel times: the
9 case of Calgary emergency medical services. *Management Science*, Vol. 56, No. 4, 2010,
10 pp. 716–723.
- 11 4. Ayamga, M., S. Akaba, and A. A. Nyaaba, Multifaceted applicability of drones: A review.
12 *Technological Forecasting and Social Change*, Vol. 167, 2021, p. 120677.
- 13 5. Nyaaba, A. A. and M. Ayamga, Intricacies of medical drones in healthcare delivery: Im-
14 plications for Africa. *Technology in Society*, Vol. 66, 2021, p. 101624.
- 15 6. Leonard, M., *Amazon Prime Air gets FAA clearance for drone delivery on 'highly*
16 *rural' test range*, 2020, [https://www.supplychaindive.com/news/amazon-prime-air-faa-](https://www.supplychaindive.com/news/amazon-prime-air-faa-clearance-drone-delivery-rural-test-range/584436/)
17 [clearance-drone-delivery-rural-test-range/584436/](https://www.supplychaindive.com/news/amazon-prime-air-faa-clearance-drone-delivery-rural-test-range/584436/), last accessed on 7/13/2021.
- 18 7. FAA, *Unmanned Aircraft Systems (UAS) BEYOND*, 2021,
19 https://www.faa.gov/uas/programs_partnerships/beyond/, last accessed on 7/13/2021.
- 20 8. Glick, T. B., M. Figliozzi, and A. Unnikrishnan, A Case Study of Drone Delivery Reli-
21 ability for Time-Sensitive Medical Supplies with Stochastic Demand and Meteorological
22 Conditions. *Transportation Research Record*, 2021, in press.
- 23 9. Bertsimas, D. and M. Sim, The price of robustness. *Operations research*, Vol. 52, No. 1,
24 2004, pp. 35–53.
- 25 10. Schmid, V. and K. F. Doerner, Ambulance location and relocation problems with time-
26 dependent travel times. *European journal of operational research*, Vol. 207, No. 3, 2010,
27 pp. 1293–1303.
- 28 11. Erdoğan, G., E. Erkut, A. Ingolfsson, and G. Laporte, Scheduling ambulance crews for
29 maximum coverage. *Journal of the Operational Research Society*, Vol. 61, No. 4, 2010,
30 pp. 543–550.
- 31 12. Azizan, M. H., C. S. Lim, W. L. W. Hatta, and L. C. Gan, Application of openstreetmap
32 data in ambulance location problem. In *2012 Fourth International Conference on Compu-*
33 *tational Intelligence, Communication Systems and Networks*, IEEE, 2012, pp. 321–325.
- 34 13. Enayati, S., M. E. Mayorga, H. K. Rajagopalan, and C. Saydam, Real-time ambulance
35 redeployment approach to improve service coverage with fair and restricted workload for
36 EMS providers. *Omega*, Vol. 79, 2018, pp. 67–80.
- 37 14. Erkut, E., A. Ingolfsson, and G. Erdoğan, Ambulance location for maximum survival.
38 *Naval Research Logistics (NRL)*, Vol. 55, No. 1, 2008, pp. 42–58.
- 39 15. Zaffar, M. A., H. K. Rajagopalan, C. Saydam, M. Mayorga, and E. Sharer, Coverage,
40 survivability or response time: A comparative study of performance statistics used in am-
41 bulance location models via simulation–optimization. *Operations research for health care*,
42 Vol. 11, 2016, pp. 1–12.
- 43 16. Naoum-Sawaya, J. and S. Elhedhli, A stochastic optimization model for real-time ambu-
44 lance redeployment. *Computers & Operations Research*, Vol. 40, No. 8, 2013, pp. 1972–
45 1978.

- 1 17. Aringhieri, R., M. E. Bruni, S. Khodaparasti, and J. T. van Essen, Emergency medical ser-
2 vices and beyond: Addressing new challenges through a wide literature review. *Computers*
3 *& Operations Research*, Vol. 78, 2017, pp. 349–368.
- 4 18. Başar, A., B. Çatay, and T. Ünlüyurt, A taxonomy for emergency service station location
5 problem. *Optimization letters*, Vol. 6, No. 6, 2012, pp. 1147–1160.
- 6 19. Li, X., Z. Zhao, X. Zhu, and T. Wyatt, Covering models and optimization techniques for
7 emergency response facility location and planning: a review. *Mathematical Methods of*
8 *Operations Research*, Vol. 74, No. 3, 2011, pp. 281–310.
- 9 20. Pulver, A., R. Wei, and C. Mann, Locating AED enabled medical drones to enhance car-
10 diac arrest response times. *Prehospital Emergency Care*, Vol. 20, No. 3, 2016, pp. 378–
11 389.
- 12 21. Pulver, A. and R. Wei, Optimizing the spatial location of medical drones. *Applied geogra-*
13 *phy*, Vol. 90, 2018, pp. 9–16.
- 14 22. Chauhan, D., A. Unnikrishnan, and M. Figliozzi, Maximum coverage capacitated facility
15 location problem with range constrained drones. *Transportation Research Part C: Emerg-*
16 *ing Technologies*, Vol. 99, 2019, pp. 1–18.
- 17 23. Chauhan, D. R., A. Unnikrishnan, M. Figliozzi, and S. D. Boyles, Robust maximum cov-
18 erage facility location problem with drones considering uncertainties in battery availability
19 and consumption. *Transportation Research Record*, Vol. 2675, No. 2, 2021, pp. 25–39.
- 20 24. Garner, A. A. and P. L. van den Berg, Locating helicopter emergency medical service bases
21 to optimise population coverage versus average response time. *BMC emergency medicine*,
22 Vol. 17, No. 1, 2017, p. 31.
- 23 25. Røislien, J., P. L. van den Berg, T. Lindner, E. Zakariassen, K. Aardal, and J. T. van Essen,
24 Exploring optimal air ambulance base locations in Norway using advanced mathematical
25 modelling. *Injury prevention*, Vol. 23, No. 1, 2017, pp. 10–15.
- 26 26. Ballou, R. H., Dynamic warehouse location analysis. *Journal of Marketing Research*,
27 Vol. 5, No. 3, 1968, pp. 271–276.
- 28 27. Nickel, S. and F. S. da Gama, Multi-period facility location. In *Location science*, Springer,
29 2015, pp. 289–310.
- 30 28. Vatsa, A. K. and S. Jayaswal, Capacitated multi-period maximal covering location problem
31 with server uncertainty. *European Journal of Operational Research*, Vol. 289, No. 3, 2021,
32 pp. 1107–1126.
- 33 29. Kim, D., K. Lee, and I. Moon, Stochastic facility location model for drones considering
34 uncertain flight distance. *Annals of Operations Research*, Vol. 283, No. 1, 2019, pp. 1283–
35 1302.
- 36 30. Ghelichi, Z., M. Gentili, and P. B. Mirchandani, Logistics for a fleet of drones for medical
37 item delivery: A case study for Louisville, KY. *Computers & Operations Research*, Vol.
38 135, 2021, p. 105443.
- 39 31. Ben-Tal, A., L. El Ghaoui, and A. Nemirovski, *Robust optimization*. Princeton university
40 press, 2009.
- 41 32. Bertsimas, D., D. B. Brown, and C. Caramanis, Theory and applications of robust opti-
42 mization. *SIAM review*, Vol. 53, No. 3, 2011, pp. 464–501.
- 43 33. Gabrel, V., C. Murat, and A. Thiele, Recent advances in robust optimization: An overview.
44 *European journal of operational research*, Vol. 235, No. 3, 2014, pp. 471–483.

- 1 34. Gorissen, B. L., İ. Yanıkoğlu, and D. den Hertog, A practical guide to robust optimization.
2 *Omega*, Vol. 53, 2015, pp. 124–137.
- 3 35. Goh, J. and M. Sim, Distributionally robust optimization and its tractable approximations.
4 *Operations research*, Vol. 58, No. 4-part-1, 2010, pp. 902–917.
- 5 36. Delage, E. and Y. Ye, Distributionally robust optimization under moment uncertainty with
6 application to data-driven problems. *Operations research*, Vol. 58, No. 3, 2010, pp. 595–
7 612.
- 8 37. Ben-Tal, A. and A. Nemirovski, Robust solutions of uncertain linear programs. *Operations*
9 *research letters*, Vol. 25, No. 1, 1999, pp. 1–13.
- 10 38. Philips, *Lead the way to save a life: Philips HeartStart AED*,
11 2019, [https://philipsproductcontent.blob.core.windows.net/assets/20170523/
12 5777e26b79a1438b8138a77c014ef7d9.pdf](https://philipsproductcontent.blob.core.windows.net/assets/20170523/5777e26b79a1438b8138a77c014ef7d9.pdf), last accessed on 7/13/2020.
- 13 39. Figliozi, M. A., Lifecycle modeling and assessment of unmanned aerial vehicles (Drones)
14 CO₂e emissions. *Transportation Research Part D: Transport and Environment*, Vol. 57,
15 2017, pp. 251–261.
- 16 40. Census-Bureau, U. S. and American-FactFinder, *2017 American Community Survey 5-*
17 *Year Estimates*. <https://factfinder.census.gov/>, 2018, accessed: 3/8/2020.
- 18 41. Gurobi Optimization, L., *Gurobi Optimizer Reference Manual*, 2020.
- 19 42. Mesa, J. A., J. Puerto, and A. Tamir, Improved algorithms for several network location
20 problems with equality measures. *Discrete applied mathematics*, Vol. 130, No. 3, 2003,
21 pp. 437–448.
- 22 43. Sirupa, R., Incorporating Conditional β -Mean based Equity Metric in Coverage based
23 Facility Location Problems, 2021, Master’s Thesis. Portland State University, Portland,
24 OR.